

Constitutive relationship for high temperature deformation of Al–3Cu–0.5Sc alloy

Guo-fu XU^{1,2,3}, Xiao-yan PENG¹, Xiao-peng LIANG², Xu LI¹, Zhi-min YIN^{1,3}

1. School of Materials Science and Engineering, Central South University, Changsha 410083, China;
2. State Key Laboratory of Powder Metallurgy, Central South University, Changsha 410083, China;
3. Key Laboratory of Nonferrous Metallurgical Materials Science and Engineering, Ministry of Education, Central South University, Changsha 410083, China

Received 16 April 2012; accepted 27 July 2012

Abstract: The high temperature compressive deformation behavior of Al–3Cu–0.5Sc alloy was investigated at temperatures from 350 to 500 °C, and strain rates from 0.01 to 10 s⁻¹ with the Gleeble–1500 thermo-mechanical simulator machine. The flow curves after corrections of the friction and temperature compensations were employed to develop constitutive equations. The effects of temperature and strain rate on deformation behaviors were represented by Zener-Hollomon parameter in an exponent type equation. The influence of true strain was incorporated in the constitutive equation by considering the effect of true strain on material constants. A four-order polynomial is found to be suitable to represent the influence of strain on the constitute equations.

Key words: Al–3Cu–0.5Sc alloy; constitutive relationship; high temperature deformation

1 Introduction

The research on scandium (Sc) addition in aluminum (Al) alloys has been received increasing attention over the last decade because of their interesting benefits. Most of the benefits are related to the formation of Al₃Sc particles, including Al₃Sc dispersoids and Al₃Sc precipitates [1]. The addition of Sc in pure aluminum or non-heat-treatable Al alloys has been extensively investigated [2,3]. In comparison, there are much fewer studies on the Sc addition in heat-treatable Al alloys [4]. But previous studies have shown that Sc can improve the strength of Al–3Cu alloy [5], however, as a deformed aluminum alloy, the deformation behavior is as important as the heat treatment process.

The flow stress of metals during hot deformation processes can be significantly influenced by several metallurgical phenomena such as working hardening, dynamic recovery and dynamic recrystallization. Therefore, the understanding of flow stress is of great importance in metal forming processes and the hot deformability can be improved by optimizing the process

parameters [6,7]. So far, many researches have been done on the hot deformation behaviors and microstructure evolution of Al alloys [8–10]. However, many constitutive models are based on the Arrhenius type of equation, which assume that the influence of strain on high temperature deformation behavior is insignificant. In fact, the flow stress is changed with the increase of the true strain, which is important for the high temperature deformation behavior. On the other hand, the effects of the friction and the temperature raise on the stress–strain curves are usually ignored. Since a strain-dependent parameter for the sine hyperbolic constitutive equation was introduced by SLOOFF et al [11], a revised sine hyperbolic constitutive equation was adopted by the incorporation of the strain to predict the elevated temperature flow behaviors for steel [12,13], pure titanium [14] and P/M TiAl based alloy [15].

In this work, a comprehensive constitutive model for describing the relationship among the flow stress, strain rate and temperature was proposed with the compensation of the strain, and it was used to predict the high temperature flow behaviors of the Al–3Cu–0.5Sc alloy.

2 Experimental

The composition (mass fraction) of the alloy used in the test was as follows: 3.0% Cu, 0.5% Sc and balance Al. The ingot was homogenized at 500 °C for 18 h. The specimens were cut from the ingot with dimensions of d 8 mm×12 mm. The specimens were compression deformed in the temperature range from 350 to 500 °C and the strain rate range from 0.01 to 10 s⁻¹ on the Gleeble-1500 thermo-mechanical simulator. All specimens were deformed to the total true strain of about 0.7. The specimens were induction-heated to deformation temperatures within 1 min and held for 3 min in order to obtain a stable and uniform temperature prior to the deformation.

3 Results and discussion

3.1 Friction correction

It is well known that the interfacial friction between the specimen and dies will affect the symmetrical deformation of the specimens [16]. In this work, although lubricants were used to minimize the interfacial friction, the interfacial friction becomes more and more evident with the increase of deformation. Thus, the deformation is more and more heterogeneous, leading to the drum-like shape of specimens, as shown in Fig. 1. ROEBUCK et al [17] developed a criterion for evaluating the effect of friction by a barreling coefficient, which is expressed as

$$B = \frac{hR_M^2}{h_0R_0^2} \quad (1)$$

where B is the barreling coefficient; h is the height of deformed specimens; R_M is the maximum radius of deformed specimens; h_0 and R_0 are the initial height and radius of specimens, respectively. When $1 < B \leq 1.1$, the difference between the measured flow stress and the true flow stress is small, the measured flow stress curves do not need to be corrected; when $B \geq 1.1$, the measured flow stress curves must be corrected.

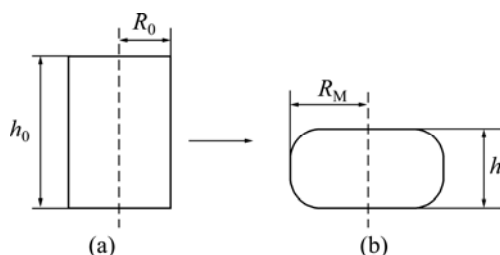


Fig. 1 Schematic plot of sample before (a) and after (b) compression

Based on the above criterion, the sizes of deformed specimens under various deformation conditions were measured, and the values of B were calculated, as shown in Table 1. From Table 1, it can be observed that all the values of B are greater than 1.1, so the measured flow stresses under all the deformation conditions must be corrected.

Table 1 Values of B under various deformation conditions

Strain rate/s ⁻¹	Value of B			
	350 °C	400 °C	450 °C	500 °C
0.01	1.16628	1.15762	1.16987	1.1744
0.1	1.11878	1.15762	1.20377	1.17143
1	1.16793	1.11878	1.12	1.17904
10	1.15967	1.18348	1.13017	1.16545

Based on the upper-bound theory, a simple theoretical analysis of the compression test for the determination of the constant friction factor (m) was proposed [18]. The base equation is shown as follows:

$$\frac{p}{\sigma} = \frac{8bR}{H} \cdot \left\{ \left[\frac{1}{12} + \left(\frac{H}{Rb} \right)^2 \right]^{3/2} - \left(\frac{H}{Rb} \right)^3 - \frac{me^{-b/2}}{24\sqrt{3}(e^{-b/2} - 1)} \right\} \quad (2)$$

where σ is the corrected true stress; p is the external pressure applied to specimens in compression (uncorrected stress); b is the barrel parameter; m is the constant friction factor; R and H are radius and height of samples, respectively, $R = R_0e^{-\epsilon/2}$ and $H = h_0e^{-\epsilon}$. m and b can be evaluated by the following equations:

$$m = \frac{R_f}{h} \cdot \frac{3\sqrt{3}b}{12 - 2b} \quad (3)$$

$$b = 4 \cdot \frac{R_M - R_T}{R_f} \cdot \frac{h}{h_0 - h} \quad (4)$$

where R_f is the average radius of samples after the deformation; R_T is the top radius of deformed samples.

$$R_f = R_0 \sqrt{\frac{h_0}{h}} \quad (5)$$

$$R_T = \sqrt{3 \cdot \frac{h_0}{h} \cdot R_0^2 - 2R_M^2} \quad (6)$$

Therefore, by this method, the corrected true stress can be calculated only by measuring the maximum radius and the height of samples after the deformation.

The true stress—true strain curves modified by considering the effects of interfacial friction are shown in Fig. 2. It can be easily found that the measured flow stress is greatly larger than the corrected ones. Meanwhile, the effect of the friction is obvious with the increase of the strain rate and the decrease of the deformation temperature.

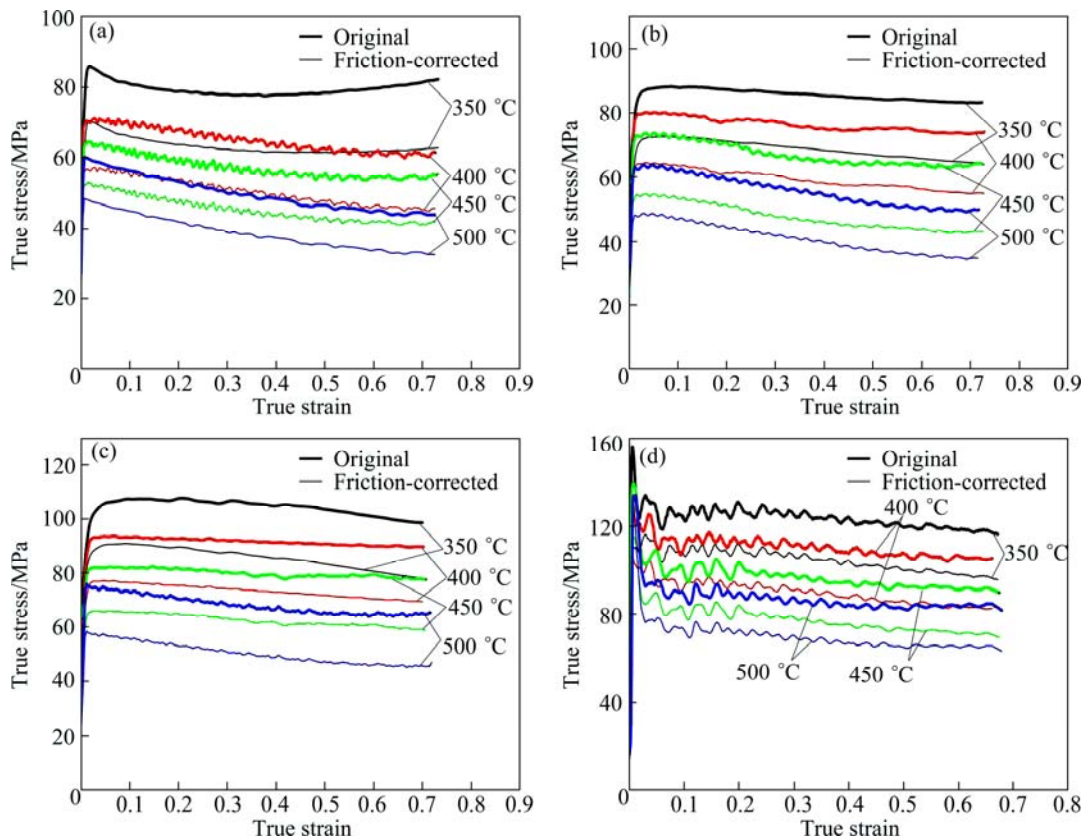


Fig. 2 Comparison between friction-corrected and measured flow stress at different strain rates: (a) 0.01 s^{-1} ; (b) 0.1 s^{-1} ; (c) 1 s^{-1} ; (d) 10 s^{-1}

3.2 Temperature correction

Flow softening is a common characteristic of stress—strain curves at high temperatures. The softening can be caused by the deformation heat or/and microstructural changes. In this compression tests, the temperature was measured and controlled by the thermocouple and computer, respectively. As the response time of the thermocouple is limited [19], the instantaneous temperature change cannot be measured while the strain rate is large enough. At the moment the deformation process is not completely isothermal, thus, the flow stress data must be corrected for the temperature rising induced by the deformation. At a strain rate of 0.001 s^{-1} , the amount of heat generated is usually very small and will be transmitted away, so the temperature corrections are conducted for high strain rate situations, with the following equation [20]:

$$\Delta T = \frac{(0.9 - 0.95)\eta \int_0^\varepsilon \sigma d\varepsilon}{\rho c_p} \quad (7)$$

where ΔT is the change of temperature; η is the adiabatic correction factor; $\int_0^\varepsilon \sigma d\varepsilon$ is the area under the uncorrected stress—strain curve (in this work, the area is under the friction-corrected stress—strain curve); ρ is the density (2.75 g/cm^3 for Al-3Cu-0.5Sc alloy); c_p is the

specific heat capacity ($0.88 \text{ J/(g}\cdot\text{K)}$ for Al-3Cu-0.5Sc alloy); the factor of (0.9–0.95) is the fraction of mechanical work transformed to heat (0.9 for Al-3Cu-0.5Sc alloy). The adiabatic correction factor η is used under the isothermal condition at strain rates $\leq 0.001 \text{ s}^{-1}$, $\eta=0$, at strain rates $\geq 10 \text{ s}^{-1}$; $\eta=1$, at strain rates between 0.001 s^{-1} and 10 s^{-1} . GOETZ and SEMIATIN [20] found that η was a complex function of the strain rate, temperature and strain, the thermal properties of workspaces and tooling, and the heat transfer coefficient at the interfaces. DADRAS and THOMAS [21] found that in the Ti-6Al-2Sn-4Zr-2Mo-0.1Si alloy, η was typically taken to vary linearly with $\lg \dot{\varepsilon}$, i.e., equaling 0.25, 0.50 and 0.75 at strain rates of 0.01, 0.1 and 1 s^{-1} , respectively.

Figure 3 shows the calculated temperature changes during the compression test at temperatures of 350, 400, 450 and $500 \text{ }^\circ\text{C}$ and strain rates of 0.01, 0.1, 1 and 10 s^{-1} , respectively. It can be seen that, at strain rates of 0.01 s^{-1} and 0.1 s^{-1} , the temperature change is small, however, at a strain rate of 1 s^{-1} and 10 s^{-1} , the temperature increase is obvious. Due to the temperature rise, especially at a strain rate of 1 s^{-1} and 10 s^{-1} , the measured flow stress curves must be corrected, which takes one of the following forms [22–24]:

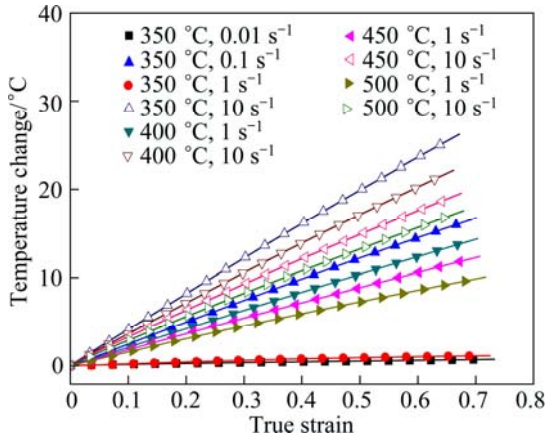


Fig. 3 Calculated temperature changes of specimens during compression test at different pre-set temperatures and strain rates

$$Z = A_1 \sigma^{n_1} = \dot{\epsilon} \exp\left(\frac{Q}{RT}\right) \quad (\text{for low stress level}) \quad (8)$$

$$Z = A_2 \exp(\beta\sigma) = \dot{\epsilon} \exp\left(\frac{Q}{RT}\right) \quad (\text{for high stress level}) \quad (9)$$

$$Z = A[\sinh(\alpha\sigma)]^n = \dot{\epsilon} \exp\left(\frac{Q}{RT}\right) \quad (\text{for all stress level}) \quad (10)$$

where Z is the Zener-Hollomon parameter; Q is the activation energy (kJ/mol); R is the universal gas constant (8.314 J/(mol·K)); T is the deformation temperature (K); A_1 , A_2 , A , β , n_1 , n and α are materials constant, $\alpha = \beta/n_1$.

In Eq. (10), α is an adjustable constant. An optimum α value can be found when the constant temperature curves in the $\ln[\sinh(\alpha\sigma)]$ against $\ln \dot{\epsilon}$ plots are almost linear and parallel with each other. In the present work, however, an optimum α value cannot be directly obtained from the uncorrected flow stress data because the specimen temperature varies at high strain rates, and the constant temperature curves cannot be plotted. In this case, the flow stress should be corrected using Eqs. (8) and (9) for low stress and high stress, respectively. The correction of flow stress for deformation heating was accomplished by plotting $\ln \sigma - T^{-1}$ curve at the low strain rate of 1 s^{-1} and plotting $\sigma - T^{-1}$ curve at the high strain rate of 10 s^{-1} , as shown in Figs. 4 and 5, respectively. Because there is no correlation of the flow stress with the strain in Eqs. (8) and (9), the correction should be made for each selected strain value.

3.3 Flow stress

Figure 6 shows the temperature corrected and friction-corrected flow stress curves of Al-3Cu-0.5Sc alloy under different experimental conditions. It can be

seen that at strain rates of 1 s^{-1} and 10 s^{-1} , however, the differences are obvious, especially at low temperatures. From Fig. 6, it can also be seen that the deformation temperature and the strain rate have a significant effect on the flow stress. At the same strain, the flow stress decreases with increasing the temperature, and rises with increasing the strain rates.

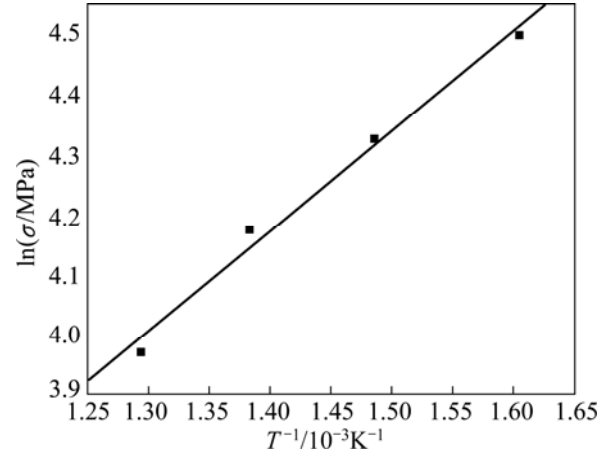


Fig. 4 Plot of $\ln \sigma - T^{-1}$ at strain of 0.2 and strain rate of 1 s^{-1}

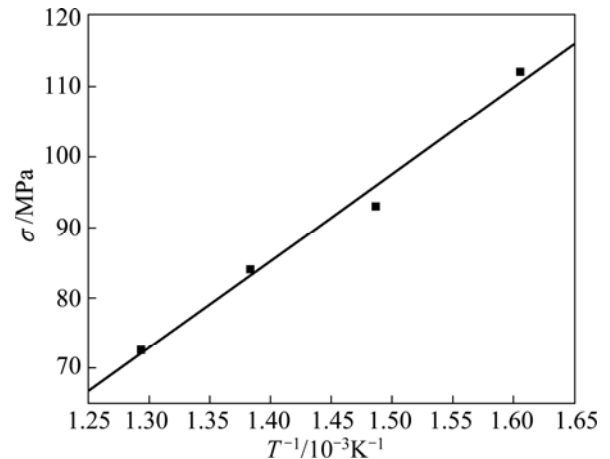


Fig. 5 Plot of $\sigma - T^{-1}$ at strain of 0.2 and strain rate of 10 s^{-1}

3.4 Determination of material constants for constitutive equation

The effect of strain on the stress is not considered in Eqs. (8)–(10), which may be reflected by the material constants in the constitutive equation. Taking the strain of 0.2 as an example, the determination of the material constants was conducted. From Eqs. (8) and (9), Eqs. (11) and (12) can be obtained:

$$\ln \dot{\epsilon} = n_1 \ln \sigma + \ln A_1 - \frac{Q}{RT} \quad (\text{for low stress level}) \quad (11)$$

$$\ln \dot{\epsilon} = \beta \sigma + \ln A_2 - \frac{Q}{RT} \quad (\text{for high stress level}) \quad (12)$$

At low stress level, an optimum n_1 value can be obtained by plotting $\ln \sigma$ against $\ln \dot{\epsilon}$ at constant temperatures, and the slope of the $\ln \sigma - \ln \dot{\epsilon}$ plot is

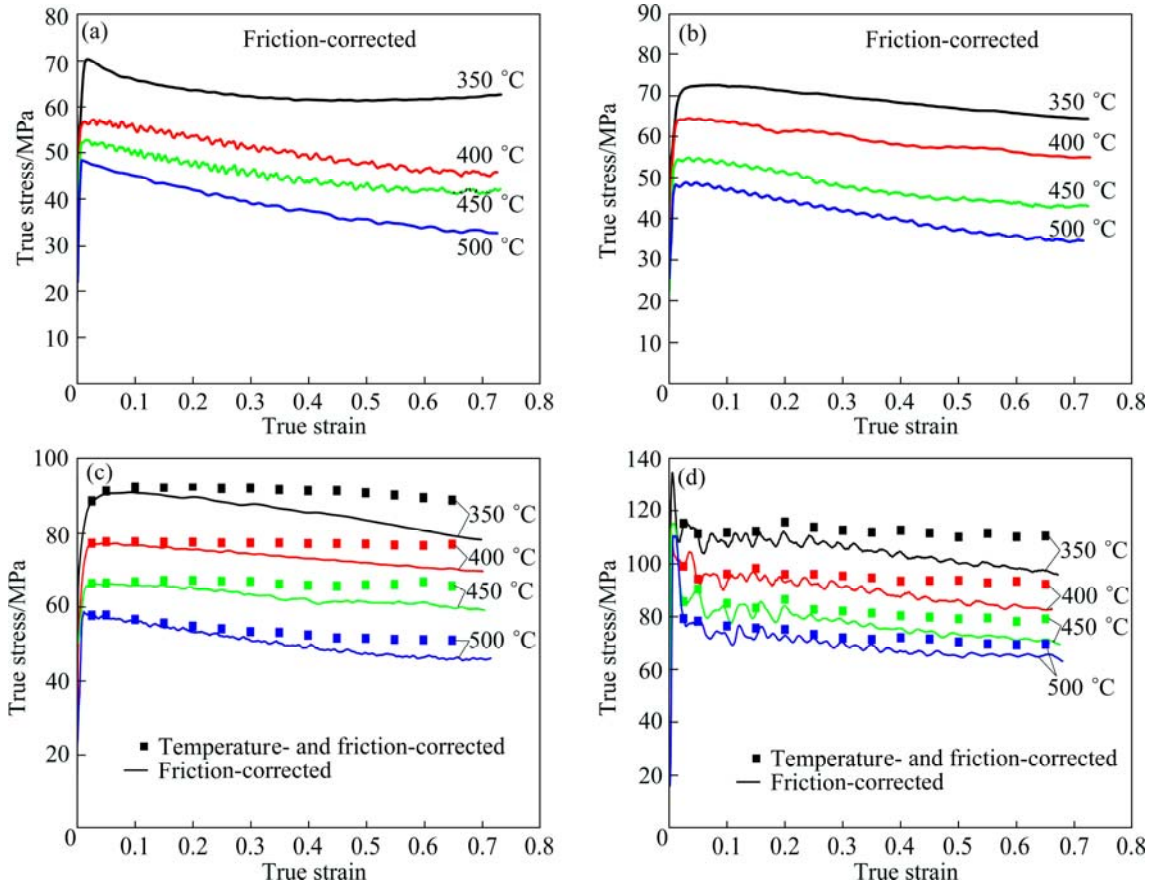


Fig. 6 Comparison between double corrected (friction- and temperature-corrected) and friction corrected flow stress at different strain rates: (a) 0.01 s⁻¹; (b) 0.1 s⁻¹; (c) 1 s⁻¹; (d) 10 s⁻¹

n_1 . At high stress level, an optimum β value can be obtained by plotting σ against $\ln \dot{\epsilon}$ at constant temperatures, and the slope of the $\sigma - \ln \dot{\epsilon}$ plot is β .

Then, substituting the corrected flow stress and corresponding strain rate at the strain of 0.2 into Eqs. (11) and (12), the relationship between the flow stress and strain rate is obtained. Because the slopes of the lines are approximately the same, the average slopes are used for deriving the values of n_1 and β , which are 10.8403975 and 0.154925 MPa⁻¹, respectively. Then, $\alpha = \beta/n_1 = 0.01429$ MPa⁻¹.

For all stress levels, Eq. (10) can be represented as follows:

$$\dot{\epsilon} = A[\sinh(\alpha\sigma)]^n \exp\left(-\frac{Q}{RT}\right) \quad (13)$$

Differentiating Eq. (13) gives:

$$Q = R \left\{ \frac{\partial \ln \dot{\epsilon}}{\partial \ln[\sinh(\alpha\sigma)]} \right\}_T \left\{ \frac{\partial \ln[\sinh(\alpha\sigma)]}{\partial (1/T)} \right\}_{\dot{\epsilon}} \quad (14)$$

From Eq. (14), it can be seen that the Q value can be derived from the slopes of $\ln \dot{\epsilon} - \ln[\sinh(\alpha\sigma)]$ and $\ln[\sinh(\alpha\sigma)] - 1/T$ plots. Substituting the values of the

corrected flow stress, deformation temperature and corresponding strain rate at the strain of 0.2 into Eq. (14). the relationships of $\ln \dot{\epsilon} - \ln[\sinh(\alpha\sigma)]$ and $\ln[\sinh(\alpha\sigma)] - 1/T$ can be obtained. Because the slopes of the lines are approximately the same, the average slopes are used to derive the activated energy, which is 133.3 kJ/mol. Then, substituting the values of Q , $\dot{\epsilon}$ and T into Eq. (10), the values of Z at different deformation temperatures and strain rates can be obtained.

Taking the natural logarithm of both sides of Eq. (10) gives:

$$\ln Z = \ln A + n \ln[\sinh(\alpha\sigma)] \quad (15)$$

The values of $\ln A$ and n are the intercept and slope of $\ln Z - \ln[\sinh(\alpha\sigma)]$ plot, respectively. By substituting the values of $\ln Z$ and corresponding corrected flow stress into Eq. (15), the relationship between $\ln Z$ and $\ln[\sinh(\alpha\sigma)]$ is shown in Fig. 7. Therefore, the values of $\ln A$ and n are determined as 21.1 and 8.102 MPa⁻¹, respectively.

3.5 Compensation of strain

It is assumed that the influence of the strain on high temperature deformation behavior is insignificant and

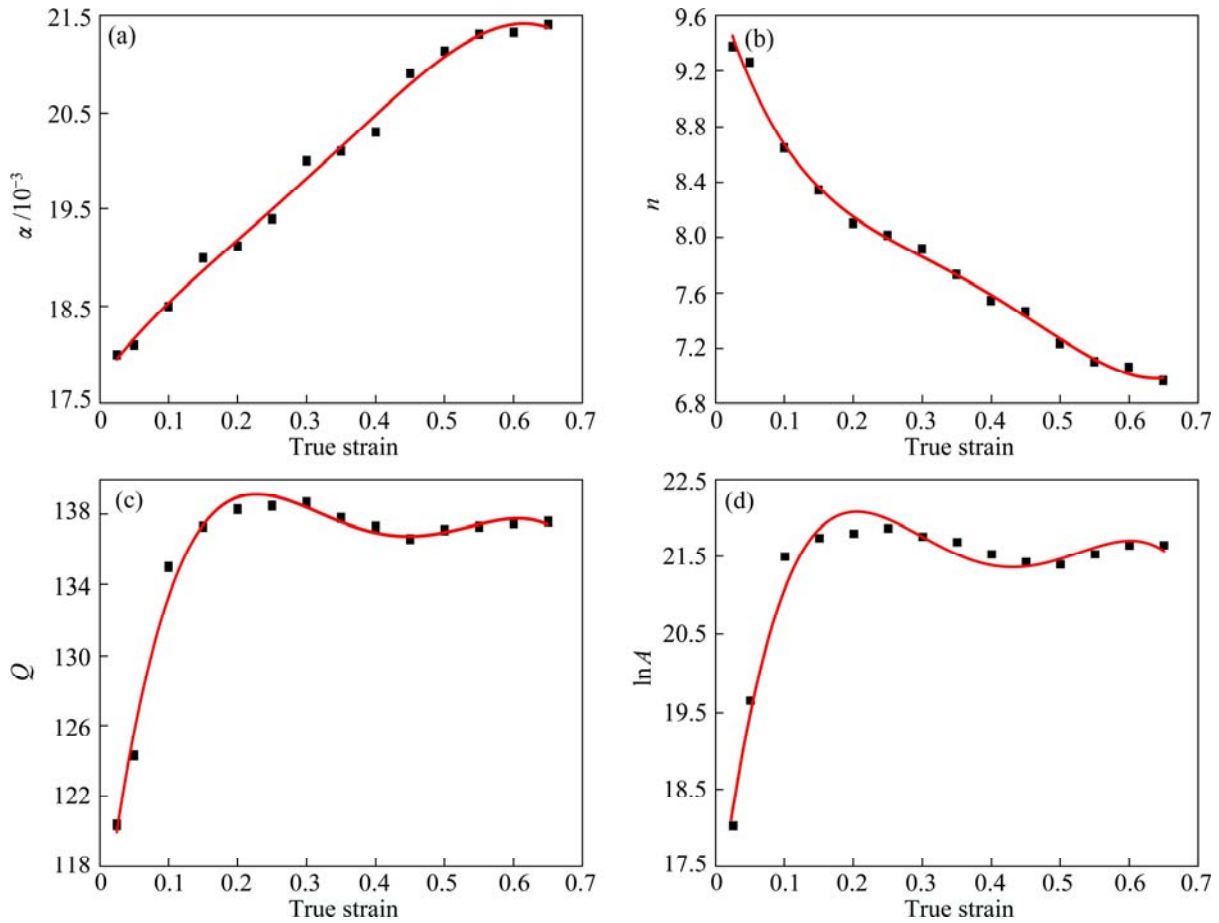


Fig. 7 Relationship between α (a), n (b), Q (c), $\ln A$ (d) and true strain by polynomial fitting of Al-3Cu-0.5Sc alloy

thereby it is not considered in Eq. (10). For the compensation of strain, the influence of strain in the constitutive equation is incorporated by assuming that the material constants (n , α , Q and A) are the polynomial function of the strain. The material constants (n , α , Q and A) of the constitutive equations were computed at various strains and an interval of 0.05. Then, these values were employed to fit the polynomial. A four-order polynomial, as shown in Eq. (16), is found to represent the influence of strain on material constants with a very good correlation for Al-3Cu-0.5Sc alloy, as shown in Fig. 7.

$$\begin{cases} \alpha = B_0 + B_1\varepsilon^1 + B_2\varepsilon^2 + B_3\varepsilon^3 + B_4\varepsilon^4 \\ n = D_0 + D_1\varepsilon^1 + D_2\varepsilon^2 + D_3\varepsilon^3 + D_4\varepsilon^4 \\ Q = E_0 + E_1\varepsilon^1 + E_2\varepsilon^2 + E_3\varepsilon^3 + E_4\varepsilon^4 \\ \ln A = F_0 + F_1\varepsilon^1 + F_2\varepsilon^2 + F_3\varepsilon^3 + F_4\varepsilon^4 \end{cases} \quad (16)$$

Once the material constants are evaluated, the flow stress at a particular strain can be predicted. The flow stress can be written as a function of Zener-Hollomon parameters. So, the proposed constitutive model can be summarized as follows:

$$\begin{cases} \sigma = \frac{1}{\alpha} \ln \left\{ \left(\frac{Z}{A} \right)^{1/n} + \left[\left(\frac{Z}{A} \right)^{2/n} + 1 \right]^{1/2} \right\} \\ Z = \dot{\varepsilon} \exp \left(\frac{Q}{RT} \right) \\ \alpha = 0.01772 + 0.00988\varepsilon - 0.02223\varepsilon^2 + \\ \quad 0.05739\varepsilon^3 - 0.05121\varepsilon^4 \\ n = 9.8258 - 16.32404\varepsilon + 58.10011\varepsilon^2 - \\ \quad 105.49637\varepsilon^3 + 68.30878\varepsilon^4 \\ Q = 112.96793 + 312.64183\varepsilon - 1294.9349\varepsilon^2 + \\ \quad 2165.25594\varepsilon^3 - 1267.76685\varepsilon^4 \\ \ln A = 16.72821 + 69.39087\varepsilon - 308.02186\varepsilon^2 + \\ \quad 540.30323\varepsilon^3 - 327.72077\varepsilon^4 \end{cases} \quad (17)$$

4 Conclusions

1) The measured flow stress of Al-3Cu-0.5Sc alloy was modified by the friction and temperature corrections,

and the friction-corrected flow stresses are lower than the measured ones. The effect of temperature on flow stress is obvious at strain rates of 10 and 1 s^{-1} .

2) The influence of strain in the constitutive analysis was incorporated by considering the effect of strain on material constants, and a four-order polynomial was found.

3) The constitutive equation considering the compensation of strain was derived.

References

- [1] CHEN B A, PAN L, WANG R H, LIU G, CHEM P M, XIAO L, SUN J. Effect of solution treatment on precipitation behaviors and age hardening response of Al–Cu alloys with Sc addition [J]. *Materials Science and Engineering A*, 2011, 530(15): 607–617.
- [2] ROBSON J D, JONES M J, PRANGNELL P B. Extension of the N-model to predict competing homogeneous and heterogeneous precipitation in Al–Sc alloys [J]. *Acta Materialia*, 2003, 51(5): 1453–1468.
- [3] FAZELI F, POOLE W J, SINCLAIR C W. Modeling the effect of Al_3Sc precipitates on the yield stress and work hardening of an Al–Mg–Sc alloy [J]. *Acta Materialia*, 2008, 56(9): 1909–1918.
- [4] KHARAKTEROVA M L, ESKIN D G, TOROPOVA L S. Precipitation hardening in ternary alloys of the Al–Sc–Cu and Al–Sc–Si systems [J]. *Acta Metallurgica Materialia*, 1994, 42(7): 2285–2290.
- [5] XU Guo-fu, NIE Zuo-ren, JIN Tou-nan, RONG Li, RUAN Hai-qiong, YIN Zhi-min. Effects of trace Sc on structures and properties of Al–3%Cu alloy [J]. *Heat Treatment of Metals*, 2004, 31(3): 24–27.
- [6] DIXIT U S, JOSHI S N, DAVIM J P. Incorporation of material behavior in modeling of metal forming and machining processes: A review [J]. *Materials and Design*, 2011, 32(7): 3665–3670.
- [7] LIN Y C, CHEN X M. A critical review of experimental results and constitutive descriptions for metals and alloys in hot working [J]. *Materials and Design*, 2011, 32(4): 1733–1759.
- [8] MOSTAFAEI M A, KAZEMINEZHAD M. Hot deformation behavior of hot extruded Al–6Mg alloy [J]. *Materials Science and Engineering A*, 2012, 535(15): 216–221.
- [9] ZHANG J, CHEN B Q, ZHANG B X. Effect of initial microstructure on the hot compression deformation behavior of a 2219 aluminum alloy [J]. *Materials and Design*, 2012, 34: 15–21.
- [10] LIN Y C, LI Q F, XIA Y C, LI L T. A phenomenological constitutive model for high temperature flow stress prediction of Al–Cu–Mg alloy [J]. *Materials Science and Engineering A*, 2012, 534(1): 654–662.
- [11] SLOOFF F A, ZHOU J, DUSZCZYK J, KATGERMAN L. Constitutive analysis of wrought magnesium alloy Mg–Al₄–Zn₁ [J]. *Scripta Materialia*, 2007, 57(8): 759–762.
- [12] XIAO Y H, GUO C. Constitutive modelling for high temperature behavior of 1Cr12Ni3Mo2VNbN martensitic steel [J]. *Materials Science and Engineering A*, 2011, 528(15): 5081–5087.
- [13] LIN Y C, CHEN M S, ZHONG J. Constitutive modeling for elevated temperature flow behavior of 42CrMo steel [J]. *Computational Materials Science*, 2008, 42(3): 470–477.
- [14] ZENG Z P, STEFAN J, ZHANG Y S. Constitutive equations for pure titanium at elevated temperatures [J]. *Materials Science and Engineering A*, 2009, 505(1–2): 116–119.
- [15] LIANG X P, LIU Y, LI H Z, ZHOU C X, XU G F. Constitutive relationship for high temperature deformation of powder metallurgy Ti–47Al–2Cr–2Nb–0.2W alloy [J]. *Materials and Design*, 2012, 37: 40–47.
- [16] LIN Y C, XIA Y C, CHEN X M, CHEN M S. Constitutive descriptions for hot compressed 2124–T851 aluminum alloy over a wide range of temperature and strain rate [J]. *Computational Materials Science*, 2010, 50(1): 227–233.
- [17] ROEBUCK B, LORD J D, BROOKS M, LOVEDAY M S, SELLARS C M, EWANS R W. Measurement of flow stress in hot axisymmetric compression tests [J]. *Materials at High Temperatures*, 2006, 23(2): 59–83.
- [18] EBRAHIMI R, NAJAFIZADEH A. A new method for evaluation of friction in bulk metal forming [J]. *Journal of Materials Processing Technology*, 2004, 152(2): 136–143.
- [19] LI L, ZHOU J, DUSZCZYK J. Determination of a constitutive relationship for AZ31B magnesium alloy and validation through comparison between simulated and real extrusion [J]. *Journal of Materials Processing Technology*, 2006, 172(3): 372–380.
- [20] GOETZ R L, SEMIATIN S L. The adiabatic correction factor for deformation heating during the uniaxial compression test [J]. *Journal of Materials Engineering and Performance*, 2001, 10(6): 710–717.
- [21] DADRAS P, THOMAS J F. Characterisation and modeling for forging deformation of Ti–6Al–2Sn–4Zr–2Mo–0.1Si [J]. *Metallurgical and Materials Transactions A*, 1981, 12(11): 1867–1876.
- [22] McQUEEN H J, RYAN N D. Constitutive analysis in hot working [J]. *Materials Science and Engineering A*, 2002, 322(1–2): 43–63.
- [23] MIRZADEHA H, CABRERA J M, PRADO J M, NAJAFIZADEH A. Hot deformation behavior of a medium carbon microalloyed steel [J]. *Materials Science and Engineering A*, 2011, 528(10–11): 3876–3882.
- [24] ZOU D N, HAN Y, YAN D G, WANG D, ZHANG W, FAN G W. Hot workability of 00Cr13Ni5Mo₂ supermartensitic stainless steel [J]. *Materials and Design*, 2011, 32(8–9): 4443–4448.

Al–3Cu–0.5Sc 合金高温变形的本构关系

徐国富^{1,2,3}, 彭小燕¹, 梁霄鹏², 李旭¹, 尹志民^{1,3}

1. 中南大学 材料科学与工程学院, 长沙 410083;
2. 中南大学 粉末冶金国家重点实验室, 长沙 410083;
3. 中南大学 有色金属材料科学与工程教育部重点实验室, 长沙 410083

摘要: 采用 Gleeble-1500 热/力模拟试验机研究 Al–3Cu–0.5Sc 合金在温度为 350–500 °C、应变速率为 $0.01\text{--}10\text{ s}^{-1}$ 条件下的高温压缩变形行为。利用经摩擦修正和温度补偿修正后的流变应力曲线建立合金的本构方程, 温度和应变速率对变形行为的影响可使用包含 Zener-Holloman 参数的指数方程来描述。通过考虑应变对材料常数的影响, 建立包含真应变的本构方程; 其真应变对本构方程的影响规律, 可通过材料常数的四次多项式拟合来实现。

关键词: Al–3Cu–0.5Sc 合金; 本构关系; 高温变形